RESEARCH PAPER

M351-0056 is a novel low MW compound modulating the actions of the immune-checkpoint protein VISTA

Xinlei Hu [ORCID] | Chenxin Qie | Jingwei Jiang | Xiaoxue Xie | Wenting Chen | Wanmei Liu | Jun Liu

Jiangsu Key Lab of Drug Screening, China Pharmaceutical University, Nanjing, China

Correspondence
Jun Liu, Jiangsu Key Lab of Drug Screening, China Pharmaceutical University, Nanjing 210009, China.
Email: junliu@cpu.edu.cn

Funding information
Natural Science Foundation of Jiangsu Province, Grant/Award Number: BK20202009; National Natural Science Foundation of China, Grant/Award Numbers: 81673443, 81973361

Background and Purpose: The protein V-domain immunoglobulin suppressor of T-cell activation (VISTA) is a novel immune-checkpoint molecule that belongs to the B7 family and regulates a broad spectrum of immune responses. So far, low MW compounds targeting VISTA for the treatment of autoimmune diseases or inflammation, have not been identified.

Experimental Approach: We developed a homology modelling for VISTA 3D structure and subsequent virtual screening for low MW ligands binding to VISTA. Visualization of the binding postures of docked ligands with protein VISTA indicated that compound M351-0056 targeted VISTA. The biological activities of compound M351-0056 targeting VISTA were investigated in vitro using monocytes and T cells and in vivo, using mice with imiquimod-induced dermatitis.

Key Results: The K_D value of M351-0056 for human VISTA-extracellular domain was 12.60 ± 3.84 μM as assessed by microscale thermophoresis. M351-0056 decreased cytokine secretion from PBMCs or human $CD4^+$ T cells, suppressed proliferation of PBMCs and enhanced expression of $Foxp3^+$ T cells. These effects of M351-0056 modulating VISTA involved the JAK2–STAT2 pathway. Daily administration of M351-0056 ameliorated imiquimod-induced psoriasis-like dermatitis. Expression of mRNA and protein of inflammatory cytokines in psoriatic lesions was decreased after M351-0056 treatment.

Conclusion and Implications: The compound M351-0056 showed high affinity for VISTA and may modulate its immune function in vitro and in vivo. Our finding provides a lead compound for therapeutically enhancing VISTA-mediated pathways to benefit the treatment of autoimmune diseases or inflammation.

1 | INTRODUCTION

Immune checkpoints provide inhibitory signals to maintain self-tolerance and protect peripheral tissues from damage during immune responses (Greenwald, Freeman, & Sharpe, 2005; Zou & Chen, 2008). The protein, V-domain immunoglobulin suppressor of T-cell activation (VISTA, gene name Vsir) is an inhibitory B7 family immune-checkpoint molecule and plays critical roles in maintaining peripheral tolerance and immune responses with other T-cell co-inhibitory receptors such as cytotoxic T lymphocyte antigen 4 (CTLA-4), programmed death-1 (PD-1), T-cell immunoglobulin-3 (TIM3), and lymphocyte activation gene-3 (LAG3) (Chen & Flies, 2013; Greenwald et al., 2005).

VISTA is a type I transmembrane protein consisting of a single N-terminal IgV domain, an approximately 30-amino acid (aa) stalk, a transmembrane domain, and a 95-aa cytoplasmic tail. The closest homologue to VISTA within the B7 family is PD-L1, which shares 22% sequence identity. The structure of the extracellular domain (ECD) of human VISTA has been elucidated, highlighting the structural features for antibody and ligand binding (Mehta et al., 2019). The human and murine VISTA proteins share over 80% identity and display similar expression patterns (Lines, Pantazi, et al., 2014). VISTA is highly expressed on myeloid cells and tumour-infiltrating lymphocytes (i.e., macrophages and myeloid-derived suppressor cells [MDSCs]) and is also expressed on naïve $CD4^+$ and $CD8^+$ T cells, where it negatively regulates T-cell responses. Therefore, VISTA serves dual functions as a receptor and ligand (Flies, Wang, Xu, & Chen, 2011; Lines, Pantazi, et al., 2014; Wang et al., 2011). Studies of many tumour models, autoimmune disease models, and clinical samples have demonstrated an important regulatory role of VISTA and its potential as a therapeutic agent or as a combination drug target (Anderson, Joller, & Kuchroo, 2016; Andrews, Marciscano, Drake, & Vignali, 2017; Gavrieli, Sedy, Nelson, & Murphy, 2006; Janakiram et al., 2017; Lines, Sempere, Broughton, Wang, & Noelle, 2014; Yi & Chen, 2009).

The multifaceted roles of VISTA in regulating both innate and adaptive immune responses have placed VISTA as a key regulator of several types of autoimmune inflammatory diseases. VISTA knockout (KO) mice have a more severe disease phenotype in the experimental autoimmune encephalomyelitis (EAE) model of multiple sclerosis and the sle1.sle3 model of lupus (Ceeraz, Eszterhas, et al., 2017; Wang et al., 2014). VISTA deficiency exacerbated imiquimod-induced skin inflammation through IL-23/IL-17 inflammatory axis (Li et al., 2017). VISTA deficiency or treatment with an immunosuppressive VISTA monoclonal antibody (mAb) (clone 8G8) resulted in attenuated disease in the collagen II antibody-induced arthritis (CAIA) model (Ceeraz, Sergent, et al., 2017). Recently, the lead compound NSC622608 blocked VISTA signalling in vitro, enhanced T-cell proliferation, and restored T-cell activation in the presence of VISTA-expressing cancer cell lines (Gabr & Gambhir, 2020). However, low MW ligands for

What is already known

- VISTA is a novel regulator of autoimmune inflammatory diseases that belongs to the B7 family.

What this study adds

- M351-0056 has high affinity with VISTA and modulated VISTA function possibly by JAK2–STAT2 pathway.
- M351-0056 could ameliorate imiquimod-induced skin inflammation.

What is the clinical significance?

- M351-0056 enhancing VISTA-mediated pathways may benefit a novel treatment of psoriasis-like skin inflammation.

VISTA for possible treatment of autoimmune diseases or inflammation are still to be discovered.

Here, we sought to discover and develop a low MW compound targeting VISTA, which would greatly benefit the treatment of autoimmune and inflammatory disease. Approximately 130,000 SDF files of structurally diverse small molecules from chemdiv library were screened by molecular docking and virtual screening. The compound M351-0056 was identified as a low MW modulator of VISTA. Furthermore, M351-0056 decreased inflammatory cytokine levels, inhibited proliferation of T cells and enhanced conversion of human T cells into $Foxp3^+$ regulatory T cells (Tregs) in vitro. The mechanism of M351-0056 modulating VISTA was possibly through the JAK2–STAT2 pathway, as assessed by RNA-sequencing (RNA-Seq) analysis. In vivo, M351-0056 ameliorated imiquimod-induced skin inflammation in mice. Our study indicates for the first time that a low MW compound can modulate the actions of VISTA in immune responses.

2 | METHODS

2.1 | Homology modelling of protein human VISTA 3D structure

The human VISTA protein ECD without the signal peptide (162 aas, UniProt: Q9H7M9) was submitted to the COACH online server for 3D structure homology modelling.

2.2 | Virtual screening for VISTA small-molecule hit ligands

The 3D model of the human VISTA-ECD as well as the ligand-binding pockets were retrieved from the COACH online server. Approximately 130,000 SDF files of structurally diverse low MW compounds from chemdiv library (MW: 300–500, XLogP: 3–5) were converted to PDBQT format as ligands using Open Babel (Version 2.4). The grid (ligand docking search space) was maximized based on the VISTA-ECD. Then, AutoDock Vina 1.1.2 was used for the subsequent molecular docking.

For the first scoring round of the docking results, docked ligands located in the predicted ligand-binding pockets with a binding energy less than -6.0 kcal·mol^{-1} were considered as the first-round candidate VISTA ligands. The best 20 candidate ligands were selected for the subsequent experimental protein–ligand interaction verification by ELISA. Once the hit ligands were verified, their docked positions were referenced as the potential ligand-binding pocket for the second-round scoring, and the other ligand-binding pockets predicted by COACH were discarded. For the second-round scoring of the docking results, docked ligands located in the potential binding pocket (the first-round hit ligands verified by the protein–ligand interaction experiment) with binding energies lower than those of the first-round hit ligands were considered as the second-round candidate VISTA ligands. The best 20 candidate ligands were selected for the subsequent experimental protein–ligand interaction verification. The hit ligands verified by the above two scoring rounds with the best binding rate (ELISA) were applied further for the VISTA-targeted biological experiments in vitro and in vivo.

2.3 | Visualization of docked ligands with the VISTA protein

Protein–ligand interactions were visualized using PyMOL (RRID: SCR_000305) Version 1.7.4.5. The aa residues of the human/mouse VISTA proteins close to the hit ligands (≤1 Å) were highlighted as potential interactive residues involved in the protein–ligand interaction. Human VISTA was structurally aligned against mouse VISTA for 3D structural comparison, which showed the structural similarities between the two VISTA proteins as well as the ligand-binding aas for the ligands.

2.4 | Microscale thermophoresis experiments

Human VISTA-ECD-his protein was labelled following the protocol provided in the Monolith NT™ Protein Labeling Kit RED-NHS (NanoTemper Technologies GmbH). M351-0056 was prepared in up to 16 serial dilutions and mixed with the labelled protein in the same volume. Then, the mixtures were incubated at room temperature for 30 min in the dark. Capillary forces were used to introduce the samples into the microscale thermophoresis capillaries. The samples were placed on a tray that was inserted into the instrument. A fluorescence scan was performed across the capillaries to determine the position of the capillaries with micrometer precision. After scanning, 16 subsequent thermophoresis measurements were performed to determine the binding affinity.

2.5 | Cell culture and reagents

Jurkat E6.1 (CLS Cat# 300223/p849_Jurkat_E61, RRID: CVCL_0367) were cultured in RPMI 1640 medium (Biological Industries) supplemented with 10% (v/v) heat-inactivated FBS (Biological Industries) and penicillin–streptomycin (100-U·ml^{-1} penicillin and 100-µg·ml^{-1} streptomycin; Biological Industries) in an atmosphere containing 5% CO_2 at 37°C. Peripheral blood mononuclear cells (PBMCs) were purchased from AllCells and were used immediately after resuscitation; these cells cannot be subcultured. Human CD4$^+$ T cells were isolated from PBMCs using an EasySep™ human CD4$^+$ T-cell isolation kit (Stem Cell) according to the manufacturer's protocol, and cultured in complete RPMI 1640 medium. All cell lines were regularly tested for mycoplasma contamination.

Total murine CD4$^+$ T cells were isolated from the spleen of wild-type (WT) mice or VISTA KO mice using an EasySep murine CD4$^+$ T-cell isolation kit (Stem Cell). The CD4$^+$ T-cell purity of 90% was used for the following experiments. The cells were cultured in complete RPMI 1640 medium supplemented. Jurkart-overexpressed VISTA or empty vector (EV) cells were constructed by lentivirus transfection. The construction of cell lines was entrusted to Hanbio Biotechnology Co., Ltd. First, pSPAX2 (RRID: Addgene_12260) (10 µg), pMD2.G (RRID: Addgene_12259) (5 µg), and human VISTA plasmid (10 µg) were transfected into HEK 293T (ATCC Cat# CRL-3216, RRID: CVCL_0063) cells by LipoFilter™ that obtain lentiviruses of EV and VISTA, and the titres were 4×10^8 and 3×10^8 TU·ml^{-1}. Then, we used the virus (MOI = 3) and polybrene (7 µg·ml^{-1}; Sangon, Shanghai) to infect Jurkat cells. When the cell density reached 60%, a medium containing puromycin (1 µg·ml^{-1}; Sangon, Shanghai) was added, for resistance screening. Cell lines have high survival rate and no pollution.

2.6 | In vitro plate-bound T-cell activation assay

For Jurkat cell cultures, 96-well flat-bottom plates were coated with the human VISTA-ECD protein at 0 or 2.5 µg·ml^{-1} in PBS at 4°C overnight. Jurkat cells were plated at a density of 2×10^4 cells per well in complete RPMI medium. A titrated amount of phytohemagglutinin (PHA, 6 µg·ml^{-1}, Sigma) and phorbol-12-myristate-13-acetate (PMA, 1 µg·ml^{-1}, Beyotime) with or without M351-0056 was added to the culture medium. Jurkat cells were treated with M351-0056 for 48 h.

For PBMCs or human CD4$^+$ T-cell cultures, 96-well flat-bottom plates were coated with anti-human CD3 (clone OKT3, BioLegend Cat# 317301, RRID: AB_571926) at 2.5 µg·ml^{-1} and anti-human CD28 (clone CD28.2, BioLegend Cat# 302901, RRID: AB_314303)

at 2.5 μg·ml^{-1} mixed together with 0, 2.5, or 5 μg·ml^{-1} of the human VISTA-ECD protein in PBS at 4°C overnight. The PBMCs or human CD4$^+$ T cells were plated at a density of 1×10^5 cells per well in complete RPMI medium. A titrated amount of M351-0056 was added to the culture medium. The cell supernatants were harvested at 48 h.

Purified CD4$^+$ T cells (100,000 cells per well) were cultured in 96-well flat-bottom plates in the presence of anti-CD3 (clone 2C11; BioLegend Cat# 10031, RRID: AB_312666, 2.5 μg·ml^{-1}) and anti-mouse VISTA antibody (clone: MH5A; Thermo Fisher Scientific Cat# 16-5919-025, RRID: AB_2866099, 10 μg·ml^{-1}). Murine CD4$^+$ T cells were stimulated for 30 min, and compound M351-0056 (10 μM) was added to the culture medium. The cell supernatants were harvested at 72 h for the cytokine secretion assay. Cells were randomly assigned to treatment groups, and the experimenter was blinded to drug treatment until data analysis has been performed.

2.7 | Cytokine measurement

For Jurkat cells, the cell supernatant was collected 48 h later, and human IL-2 was detected by ELISA (BioLegend). Supernatant from the PBMCs, human, or mouse CD4$^+$ T-cell costimulation assays was collected at 2, 12, 24, 48, or 72 h. Human IFN-γ, IL-2, IL-17A and TNF-α were detected by ELISA (BioLegend).

2.8 | Cell proliferation assay

PBMCs were labelled with 5-(and 6)-carboxyfluorescein diacetate succinimidyl ester (CFSE) following the manufacturer's protocol (BioLegend). Briefly, cells were labelled at 10^6 cells·ml^{-1} at 37°C for 10 min with 5-mmol·L^{-1} CFSE in PBS containing 0.1% BSA. CFSE was quenched by adding twice the volume of complete media, followed by three washes in complete media. PBMCs were stimulated with anti-human CD3 antibodies (BioLegend, Cat# 317301, RRID: AB_571926). Cell proliferation was analysed on Day 5 for CFSE profiles by flow cytometry.

2.9 | Flow cytometry

For staining following culture, PBMCs were harvested and washed with FACS staining buffer (eBioscience) and then stained with antibodies for extracellular markers. Antibodies against CD4 (BD Biosciences, Cat# 561005; RRID: AB_10561684) were purchased from BD Biosciences. To stain intranuclear Foxp3, we used the Foxp3 Fixation/Permeabilization Concentrate and Diluent Kit from eBioscience according to the manufacturer's directions and anti-Foxp3 clone 236A/E7 (BD Biosciences, Cat# 560852, RRID: AB_10563418) from BD Biosciences. Samples were acquired on BD C6 Flow cytometry and analysed with FlowJo V10 software (FlowJo, RRID: SCR_008520).

2.10 | RNA sequencing

PBMCs were harvested and were washed with cold PBS. Total RNA was extracted using TRIzol reagent (Vazyme). RNA sequencing was undertaken commercially by ChosenMed Technology Co., Ltd.

2.11 | RNA extraction and real-time PCR

Total RNA was extracted from PBMCs or skin tissue using TRIzol reagent. The RNA was transcribed to cDNA with HiScript® II Q RT SuperMix for qPCR (Vazyme) according to the manufacturer's instructions. The mRNA levels of IL-17A, IFN-γ, TNF-α, PDGF receptor alpha (PDGFRA), IL-4R, IL-21R, IFNAR1, IFNGR1, JAK2, IFN regulatory factor 9 (IRF9), STAT2, protein tyrosine phosphatase non-receptor type 2 (PTPN2), and recombinant protein inhibitor of activated STAT3 (PIAS3) were measured by real-time quantitative PCR analysis using the ABI StepOnePlus sequence detection system (Applied Biosystems). Quantitative real-time PCR was performed by using a ChamQ™ SYBR® qPCR Master Mix (High ROX Premixed) (Vazyme) according to the manufacturer's instructions. The specific primers are shown in Table 2. The expression levels of each gene were normalized against GAPDH using the comparative $2^{-\Delta\Delta CT}$ method, and the results were obtained from three independent experiments according to the manufacturer's protocols.

2.12 | Western blotting

PBMCs or mouse skin tissues were harvested and lysed in RIPA (Beyotime Institute of Biotechnology) buffer with protease inhibitor cocktail (Bimake) and phosphatase inhibitor cocktail (Bimake). p-JAK2 (Cell Signaling Technology, Cat# 3771, RRID: AB_330403), JAK2 (Cell Signaling Technology, Cat# 3230, RRID: AB_2128522), p-STAT2 (Cell Signaling Technology, Cat# 88410, RRID: AB_2800123), STAT2 (Cell Signaling Technology, Cat# 72604, RRID: AB_2799824), TNF-α (Abcam, Cat# ab1793, RRID: AB_302615), IFN-γ (Abcam, Cat# ab9657, RRID: AB_2123314), IL-1β (Abcam, Cat# ab9722, RRID: AB_308765), IL-17 (Abcam, Cat# ab79056, RRID: AB_1603584), IL-23 (Abcam, Cat# ab45420, RRID: AB_2124515), β-actin (Servicebio, Cat# GB11001, RRID: AB_2801259), and GAPDH antibody (Arigo, Cat# ARG10112, RRID: AB_2885012) were used for Western blotting. The Immuno-related procedures used comply with the recommendations made by the *British Journal of Pharmacology* (Alexander et al., 2018).

2.13 | Mice

All animal care and experimental procedures were performed in accordance with the Laboratory Animal Management Committee of

Jiangsu Province and approved by the ethics committee of China Pharmaceutical University. Animal studies are reported in compliance with the ARRIVE guidelines (Percie du Sert et al., 2020) and with the recommendations made by the *British Journal of Pharmacology* (Lilley et al., 2020). BALB/c (RRID: MGI:2683685) mice (female, 8 weeks) were purchased from Beijing Vital River Laboratory Animal Technology Co., Ltd. (Beijing, China; https://www.vitalriver.com/). C57BL/6J (RRID: IMSR_CRL:219) mice were purchased from Shanghai Model Organisms Center, Inc. (Shanghai, China; https://www.modelorg.com/en/). VISTA KO mice on a fully backcrossed C57BL/6J background were obtained from the Shanghai Model Organisms Center, Inc. (Shanghai, China; https://www.modelorg.com/en/). Mice were kept under specific pathogen-free conditions and provided with water and food ad libitum.

2.14 | Imiquimod-induced psoriasiform inflammation model

The BALB/c mice were separated into the following three groups: (i) mice in the control group (Control) were treated with control cream; (ii) mice in the model group (Model) received a daily topical dose of 62.5 mg of commercially available imiquimod cream (5%); and (iii) mice in M351-0056 group were treated with M351-0056 (25 mg·kg^{-1}·day^{-1}; p.o.). All these treatments were continued for six consecutive days, on the right ear and the shaved back. The ear thickness was measured using a micrometer every day. For histopathological analysis, haematoxylin and eosin (H&E) staining was performed on 4% formalin-fixed, paraffin-embedded skin samples. Sections of skin were photographed at an objective magnification of ×20 using a microscope (BX53, Olympus, Tokyo, Japan). Animals were randomly assigned to treatment groups, and the experimenter was blinded to drug treatment until data analysis has been performed.

2.15 | Data and statistical analysis

The data analysis was performed in a blinded manner. The data are expressed as the mean ± SD unless indicated otherwise. The sample size was $n = 8$ per group in animal experiments and $n = 5$ per group in other experiments, and outliers were included in data analysis and presentation. Group size is the number of independent values, and statistical analysis was done using these independent values. An unpaired Student's t test or one-way ANOVA with Bonferroni's post hoc test, while post hoc tests were run only if F achieved $P < .05$ and there was no significant variance inhomogeneity, was used to determine statistically significant differences. For data that did not pass normality testing, log transformation was applied to generate Gaussian-distributed data set that could be subjected to parametric statistical analysis or non-parametric statistics were used (Wilcoxon rank-sum test or Kruskal–Wallis H test). A value of $P < .05$ was considered significant at the 95%

confidence level and was considered statistically significant; the P value is not varied later in Section 3. Analyses were performed using GraphPad Prism 8 (GraphPad Prism, RRID: SCR_002798) unless otherwise indicated. The data and statistical analysis comply with the recommendations of the *British Journal of Pharmacology* on experimental design and analysis in pharmacology (Curtis et al., 2018).

2.16 | Materials

M351-0056 was synthesized and provided by Hebei Sundia MediTech Company, Ltd (Hebei, China). Imimiquod (5%) cream was supplied by Sichuan MED-SHINE Pharmaceutical Co.Ltd (Sichuan, China).

2.17 | Nomenclature of targets and ligands

Key protein targets and ligands in this article are hyperlinked to corresponding entries in the IUPHAR/BPS Guide to PHARMACOLOGY (http://www.guidetopharmacology.org) and are permanently archived in the Concise Guide to PHARMACOLOGY 2019/20 (Alexander et al., 2019).

3 | RESULTS

3.1 | Virtual screening for low MW hit ligands for VISTA

To identify compounds binding to VISTA, the homology modelling of the VISTA 3D structure was set up, and virtual screening for low MW hit ligands for VISTA was carried out. After two-round virtual screening, 20 candidate compounds were identified and their binding with protein VISTA-ECD was determined by ELISA. Two compounds (M351-0056 and M351-0110) were identified as lead compounds (Table S1). The predicted binding energies for the two compounds showed good binding affinity for human VISTA-ECD protein. The interactions of protein VISTA-ECD and its ligand were visualized with the PyMOL software and displayed. The docked positions of the two modulators as well as their interacting residues are shown in Figure 1a,b. The docked parameters of these protein–ligand interactions are summarized in Table 1. In the subsequent experiments, we chose M351-0056 (Figure 1c) to confirm its biological actions mediated through VISTA.

3.2 | The K_D value of the compound M351-0056 for the protein VISTA-ECD

In order to investigate the biological activities of M351-0056 on VISTA, the recombinant protein human VISTA-ECD was expressed
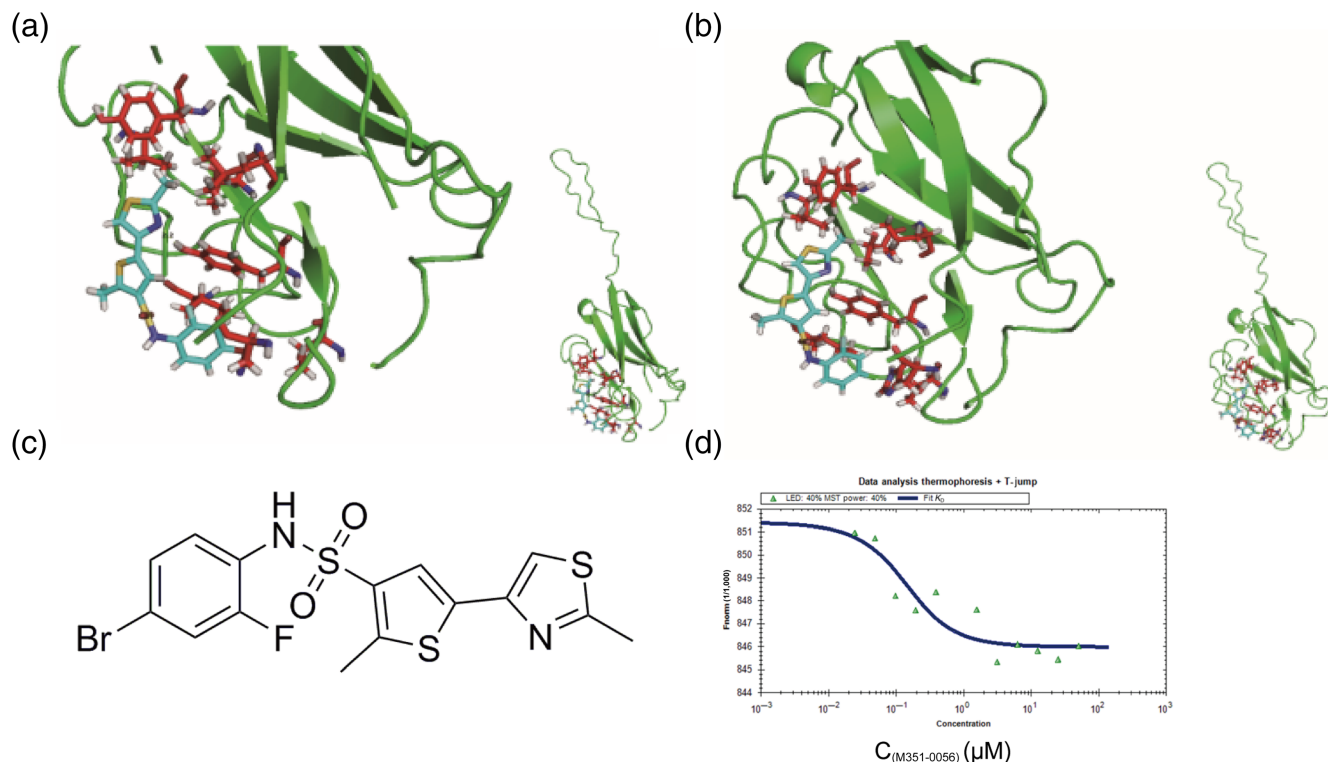
(a)

(b)

(c)

(d)

$C_{(M351-0056)}$ (μM)

FIGURE 1 The ligands (light blue) interacting with local residues of the protein human VISTA-ECD (green). Residues on the VISTA protein interacting with ligands are highlighted in red. The bottom right images of (a) and (b) show the whole VISTA protein extracellular domain and the docked positions of each ligand. Hydrogen bonds between the ligand and residues are highlighted with a yellow dashed line. (a) M351-0056 binding with protein human VISTA-ECD. (b) M351-0110 binding with protein human VISTA-ECD. (c) The structure of compound M351-0056. (d) Binding affinity was detected between human VISTA-ECD protein and M351-0056 by microscale thermophoresis procedures

TABLE 1 The docked parameters of M351-0056 and M351-0110 interaction with human VISTA-ECD protein

Macromolecule	Hit ligand	Hydrogen bonds	Potential hydrophobic interactions	Predicted binding energy (kcal·mol^{-1})
Human VISTA	M351-0056	TYR37	THR67, TYR69, THR71, TYR73, VAL80, ILE89, IEU147, HIS155	−7.3
Human VISTA	M351-0110	NA	THR67, TYR69, THR71, TYR73, VAL80, ILE89, IEU147, HIS155	−7.5

by CHO system and purified from the cell supernatant using Ni Sepharose™ 6 Fast Flow resin (GE Healthcare). The proteins were verified by Western blotting (Figure S1). The binding characteristics of M351-0056 to VISTA were assayed by microscale thermophoresis and showed that M351-0056 had good affinity for human VISTA with a K_D value of 12.60 ± 3.84 μM (Figure 1d). The hits identified based on this approach will be a good starting point for further structural optimization in the future.

3.3 | M351-0056 inhibits VISTA function on T cells

VISTA has previously been demonstrated to suppress T-cell immune responses (Lines, Pantazi, et al., 2014), and therefore, a comprehensive

set of studies with M351-0056 on human VISTA was performed on a spectrum of human T-cell subsets to evaluate its biological activities. The levels of cytokines in PBMCs treated with VISTA and M351-0056 were determined first. PBMCs generated a large amount of IFN-γ, IL-17A, TNF-α, and IL-2 when stimulated with the anti-human CD3 and CD28 antibodies. VISTA protein suppressed the levels of IL-2, TNF-α, IL-17A, and IFN-γ. Moreover, the cytokine levels were further reduced after M351-0056 was added (Figure 2a–d). To further determine the effect of M351-0056 on VISTA, PBMCs were immobilized on 96-well plates, and human VISTA-ECD protein shown to suppress the proliferation of PBMCs in response to anti-human-CD3 stimulation. The proliferation of PBMCs was further inhibited by M351-0056 (Figure 2e). Furthermore, M351-0056 also decreased cytokine production in activated human CD4$^+$ T cells (Figure S4). Tregs play important role in maintaining the balance of immune response and inflammation
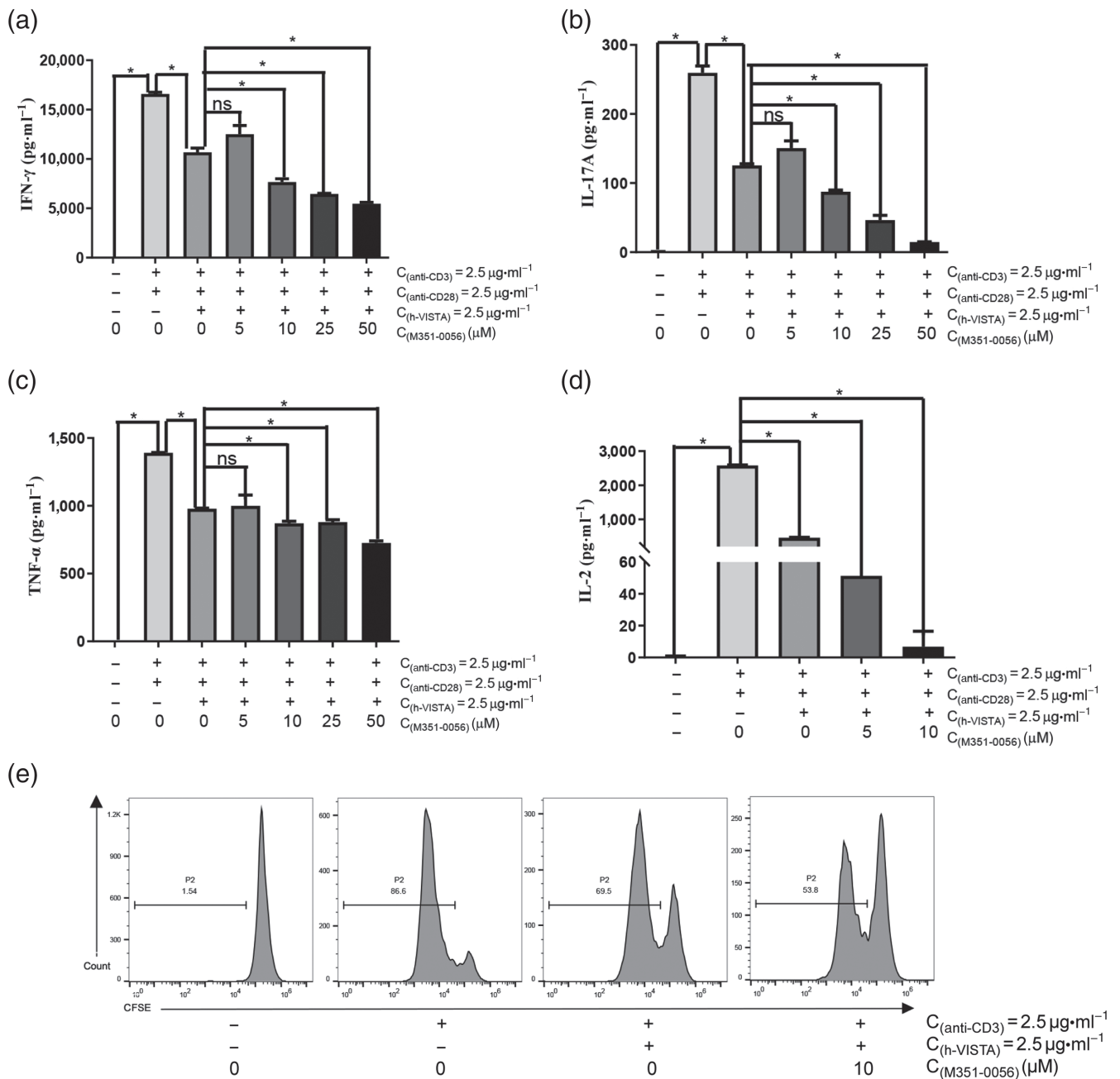
FIGURE 2   Compound M351-0056 further decreased the inhibitory effects of human VISTA-ECD protein on cytokine production and cell proliferation in human PBMCs. A total of 1×10^5 PBMCs were incubated with an immobilized anti-human CD3 antibody (2.5 $\mu g \cdot ml^{-1}$), anti-human CD28 antibody (2.5 $\mu g \cdot ml^{-1}$), and human VISTA (2.5 $\mu g \cdot ml^{-1}$), and compound M351-0056 was added as indicated. The levels of (a) IFN-γ, (b) IL-17A, (c) TNF-α, and (d) IL-2 in the cell culture supernatants were measured at 48 h using ELISA kits. (e) CFSE-labelled PBMCs were stimulated by plate-bound anti-human-CD3 (1 $\mu g \cdot ml^{-1}$) together with co-absorbed human VISTA-ECD protein (2.5 $\mu g \cdot ml^{-1}$) and compound M351-0056 (10 μM) was added. The proliferation of PBMCs were measured on Day 5 for CFSE profiles. ns, not significant. *$P <$ .05, significantly different, ns, not significant, as indicated

disease. As well as suppressing effector T-cell responses, VISTA increased the conversion of naïve T cells into Foxp3^{+} regulatory cells (Lines, Pantazi, et al., 2014). In this study, M351-0056 also further promotes the expression of human CD4^{+} Foxp3^{+} in PBMCs (Figure 3). These results indicated that M351-0056 could enhance the functions of VISTA on T cells.

3.4 | The specificity of M351-0056 in modulating VISTA

VISTA is known to suppress IL-2 secretion in Jurkat cells stimulated with PMA and PHA. Addition of M351-0056 further inhibited IL-2 production in a dose-dependent manner(25 or 50 μM) in Jurkat cells
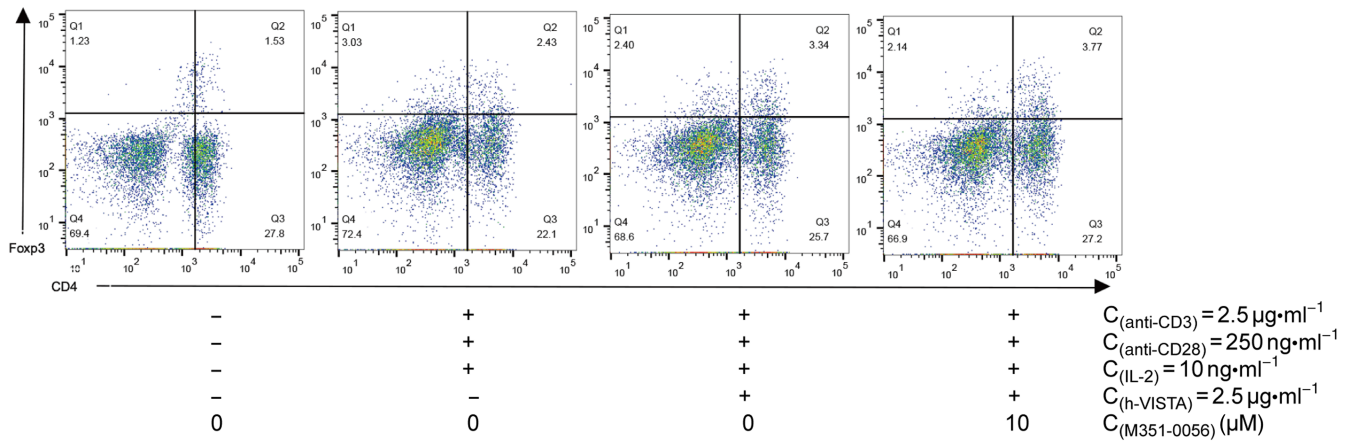
C(anti-CD3) = 2.5 μg·ml^{-1}
C(anti-CD28) = 250 ng·ml^{-1}
C(IL-2) = 10 ng·ml^{-1}
C(h-VISTA) = 2.5 μg·ml^{-1}
C(M351-0056) (μM)

FIGURE 3 Compound M351-0056 further enhanced the expression of human CD4$^+$FoxP3$^+$ in PBMCs. PBMCs (1 × 10^5) were stimulated with anti-CD3 co-coated with human VISTA-ECD (2.5-μg·ml^{-1}) in the presence of IL-2 (10 ng·ml^{-1}) and anti-CD28 (250-ng·ml^{-1}) in the culture media, and compound M351-0056 was added as indicated. Staining of PBMCs with FITC-anti-human CD4 followed by intracellular staining with PE-anti-human Foxp3 using the Foxp3 staining buffers on Day 5
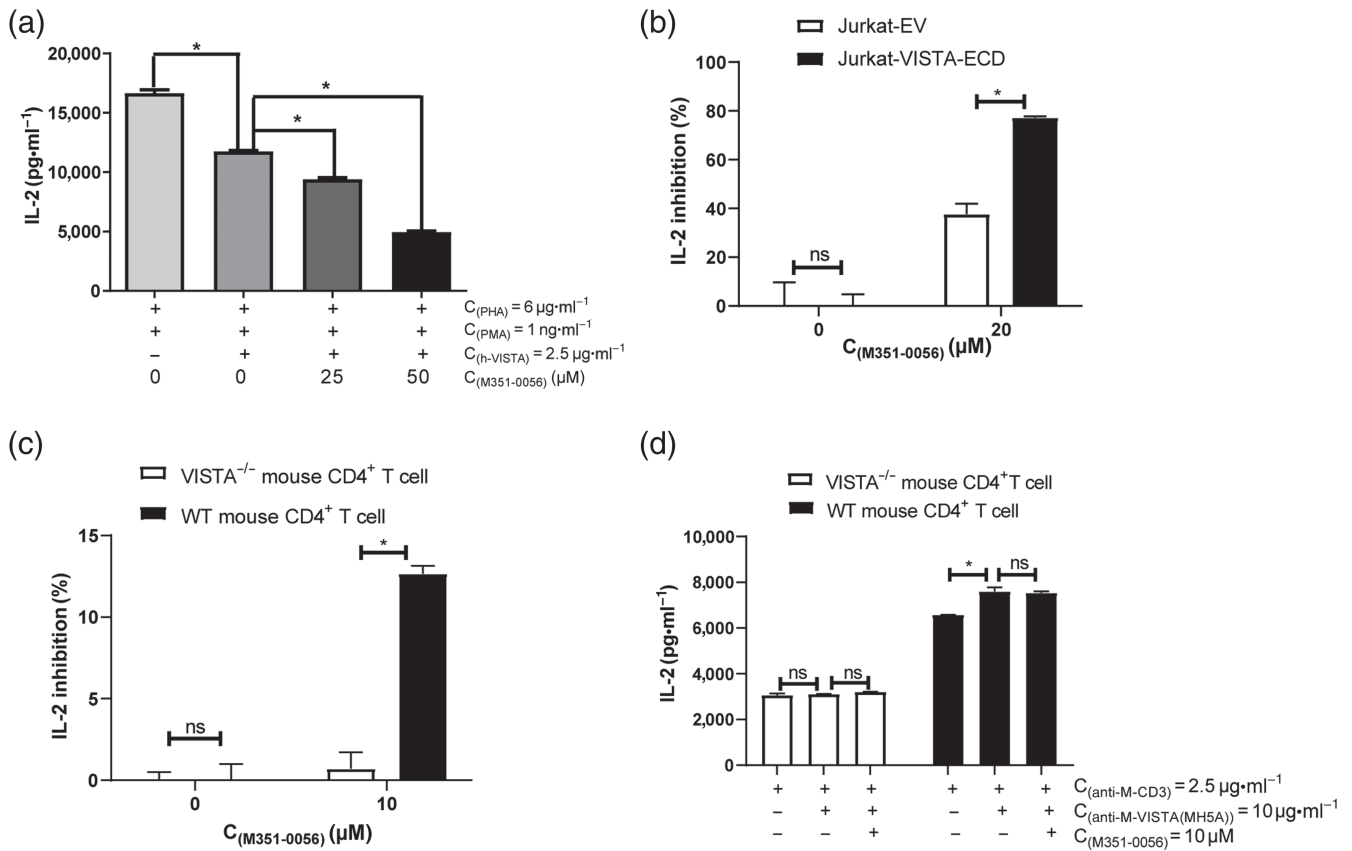

FIGURE 4 Compound M351-0056 inhibited IL-2 production in Jurkat cells and primary murine CD4$^+$ T cells. (a) The human VISTA-ECD protein (2.5 μg·ml^{-1}) was coated on 96-well flat-bottom plates. Jurkat cells (2 × 10^4 cells per well) were stimulated with PMA (1 ng·ml^{-1}) and PHA (6 μg·ml^{-1}). Different concentrations of M351-0056 were added as indicated, and culture supernatants were collected at 48 h. The IL-2 level was analysed by ELISA. (b) Jurkat cells overexpressing VISTA, (Jurkat–VISTA-ECD) or Jurkat cells expressing empty vector (Jurkat-EV cells) (2 × 10^4 cells per well) were stimulated with PMA and PHA. M351-0056 (20 μM) was added as indicated, and culture supernatants were collected at 48 h. The IL-2 level was analysed by ELISA. Purified primary murine CD4$^+$ T cells (1 × 10^5 cells per well) from spleen of WT or VISTA KO mice were cultured in 96-well flat-bottom plates in the presence of (c) anti-CD3 (2.5 μg·ml^{-1}) or (d) anti-CD3 (2.5 μg·ml^{-1}) and anti-mouse VISTA antibody (clone: MH5A; 10 μg·ml^{-1}). M351-0056 (10 μM) was added as indicated, and culture supernatants were collected at 72 h. The IL-2 level was analysed by ELISA. *P < .05, significantly different, ns, not significant, as indicated

(Figure 4a). To further evaluate the specificity of M351-0056 in modulating the actions of VISTA, Jurkat cells overexpressing the VISTA-ECD were constructed. The inhibition of IL-2 production by VISTA was significantly increased by M351-0056 in Jurkat cells overexpressing VISTA, compared with Jurkat cells stimulated with PHA and PMA (Figure 4a,b). These results indicate that M351-0056 was acting through VISTA.

VISTA is known to exhibit considerable homology (over 80%) across the murine and human forms of VISTA. To further study the specificity of M351-0056 on VISTA, we used murine CD4$^+$ T cells isolated from spleen of VISTA KO mice and WT mice. Addition of M351-0056 further inhibited IL-2 secretion in activated CD4$^+$ T cells from WT mice with VISTA. However, no inhibition was observed in CD4$^+$ T cells from VISTA KO mice (Figure 4c). Furthermore, we used VISTA antibody to block VISTA, and M351-0056 was added to WT CD4$^+$ T cells and VISTA KO CD4$^+$ T cells separately. The cell supernatants were harvested at 72 h for cytokine secretion assay. The results showed that VISTA antibody promotes IL-2 secretion in CD4$^+$ T cells from WT mice, while there was no significant change after adding M351-0056. However, there was no effect on IL-2 secretion by the VISTA antibody in CD4$^+$ T cells from VISTA KO mouse by M351-0056 (Figure 4d). These results suggested that M351-0056 might target VISTA on T cells.

3.5 | M351-0056 regulates VISTA immune responses by JAK2–STAT2 pathway

To explore the possible mechanisms underlying the modulation of VISTA protein by M351-0056, the RNA transcripts of from PBMCs treated with M351-0056 were sequenced. RNA sequencing revealed a differential gene expression of the JAK2–STAT2 signalling pathway (Figure 5a). The expressions of **PDGFRα**, **IL-4 receptor**, **IL-21 receptor**, **IFN-α/β receptor**1, **IFN-γ receptor1**, **JAK2**, IRF9, STAT2, PIAS3, and PTPN2 and protein expressions of p-JAK2 and p-STAT2 were measured. The results showed that the gene expressions of IL-4R, IL-21R, IFNAR1, IFNGR1, JAK2, IRF9, STAT2, and PIAS3, as well as the protein expressions of p-JAK2 and p-STAT2, were decreased after M351-0056 treatment (Figure 5b,c). These results indicate that M351-0056 restricts the activation of the JAK2–STAT2 pathway and moderately decreased the phosphorylation of JAK2–STAT2 in PBMCs.

3.6 | M351-0056 ameliorates imiquimod-induced skin inflammation in a mouse model of psoriasis and reduced cytokine expression

In the imiquimod-induced psoriasis model, VISTA deficiency augmented the inflammatory responses, resulting in exacerbated psoriasiform dermatitis (Li et al., 2017). In this study, M351-0056 decreased the imiquimod-induced skin inflammation in mice that phenotypically resembles psoriasis (Figure 6a) and reduced ear

thickness (Figure 6b). H&E results showed that M351-0056 decreased ear and back thickness (Figure 6c–e). To investigate the inflammatory milieu, mRNA from imiquimod -treated mouse skin was examined by quantitative RT-PCR. The results showed that M351-0056 decreased the mRNA levels of cytokines (IFN-γ, TNF-α, IL-17A, and IL-1β) in mouse lesion skin, compared with the model group (Figure S5). Protein levels of IFN-γ, TNF-α, IL-17A, and IL-1β in serum were higher in the model group receiving only imiquimod treatment, and were decreased significantly after M351-0056 treatment (Figure 6f–i). Protein levels of pro-inflammatory factors in mouse lesion skin and control skin were measured by western blotting and showed that levels of IFN-γ, TNF-α, IL-1β, IL-17, and IL-23 in the model group were significantly increased. These increased levels were reduced after oral administration of M351-0056. Thus, M351-0056 exerted a therapeutic effect on the inflammation in psoriasis-like skin (Figure 7). Together, these results indicate that M351-0056 decreased the expression of inflammatory cytokines in response to imiquimod (Table 2).

4 | DISCUSSION

VISTA is a novel immunoregulatory protein with broad expression on both the lymphocyte and myeloid compartments at steady state, which plays a unique and important homeostatic role in the immune system (ElTanbouly et al., 2020). VISTA regulates a broad spectrum of autoimmune and inflammatory diseases, including EAE, lupus, and psoriasiform inflammation. Of note, reduced VISTA expression under inflammatory conditions has been detected by many groups (Bharaj et al., 2014; Borggrewe et al., 2018; ElTanbouly et al., 2020). Targeting VISTA with modulators will greatly benefit the treatment of autoimmune and inflammatory diseases. However, there are no low MW compounds reported to modulate the actions of VISTA in regulating inflammation.

In this study, we conducted homologous modelling of the human VISTA-ECD protein, with I-TASSER software. Comparing the recently published crystal structure of VISTA-ECD (PDB code: 6oil) (Mehta et al., 2019) with a corresponding VISTA homologous reconstructed model we constructed 2 years ago, we had obtained a very precise virtual VISTA 3D model (root mean SD = 3.6 Å, structurally aligned to 6oil) (He, Liu, Luo, Zhang, & Jiang, 2020). Based on this model, we have successfully screened modulators for protein VISTA without any published 3D structure 2 years ago. As a result, M351-0056 was been discovered as a low MW hit ligand for VISTA.

ExpiCHO cells were used to express the human VISTA-ECD and obtain high purity human VISTA protein by affinity chromatography (Figure S1). The K_D value of M351-0056 for human VISTA-ECD was 12.60 ± 3.84 μM, as shown by microscale thermophoresis. The T-cell activity experiments revealed that M351-0056 significantly stimulated VISTA targets and further inhibited IL-2 secretion with VISTA in activated Jurkat cells, PBMCs, and human CD4$^+$ T cells. We also performed cytometric bead array assays to determine the effect of M351-0056 on inflammatory cytokine secretion by PBMCs. The
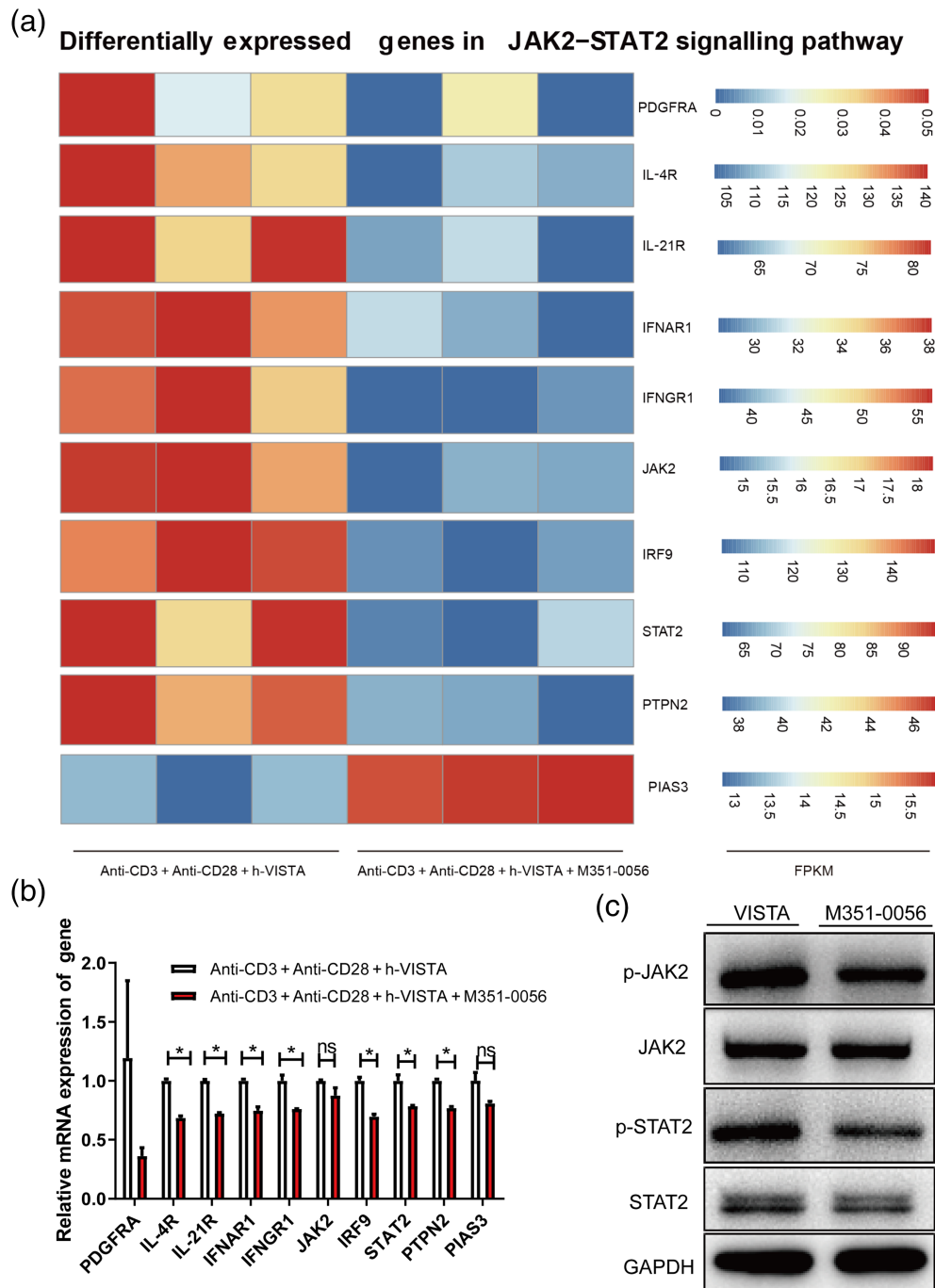
FIGURE 5 M351-0056 regulated VISTA function through JAK2–STAT2 signalling pathway. (a) Heatmap showing the results of the RNA-Seq data analyses. (b) The expression of mRNA for PDGFRα (PDGFRA), and receptors for IL-4 (IL-4R), IL-21 (IL-21R), IFN-α (IFNAR1) and IFN-γ (IFNGR1), JAK2, IRF9, STAT2, PIAS3, and PTPN2 were analysed by qRT-PCR in PBMC cells. (c) The protein levels of p-JAK2, JAK2, p-STAT2, and STAT2 were assayed by western blot analysis. GAPDH was used as an internal control. *$P < .05$, significantly different, ns, not significant, as indicated

results showed that M351-0056 further reduced cytokine secretion (e.g., IFN-γ, IL-2, and TNF-α) by VISTA (data not show). Furthermore, M351-0056 significantly suppresses the proliferation of PBMCs or CD4+ T cells and also further promotes the expression of Foxp3 to stabilize the persistence of the Tregs. To verify the specificity of M351-0056 on VISTA, the VISTA-overexpressed Jurkat cells, VISTA

KO cells, and VISTA antibody were also used in this study, and the results suggested that M351-0056 is indeed mediated through VISTA. Taken together, our results show that M351-0056 may be a modulator of the human VISTA-ECD protein.

Next, to explore the possible mechanism of M351-0056 on VISTA protein, the RNA-Seq analysis was performed in PBMCs. The
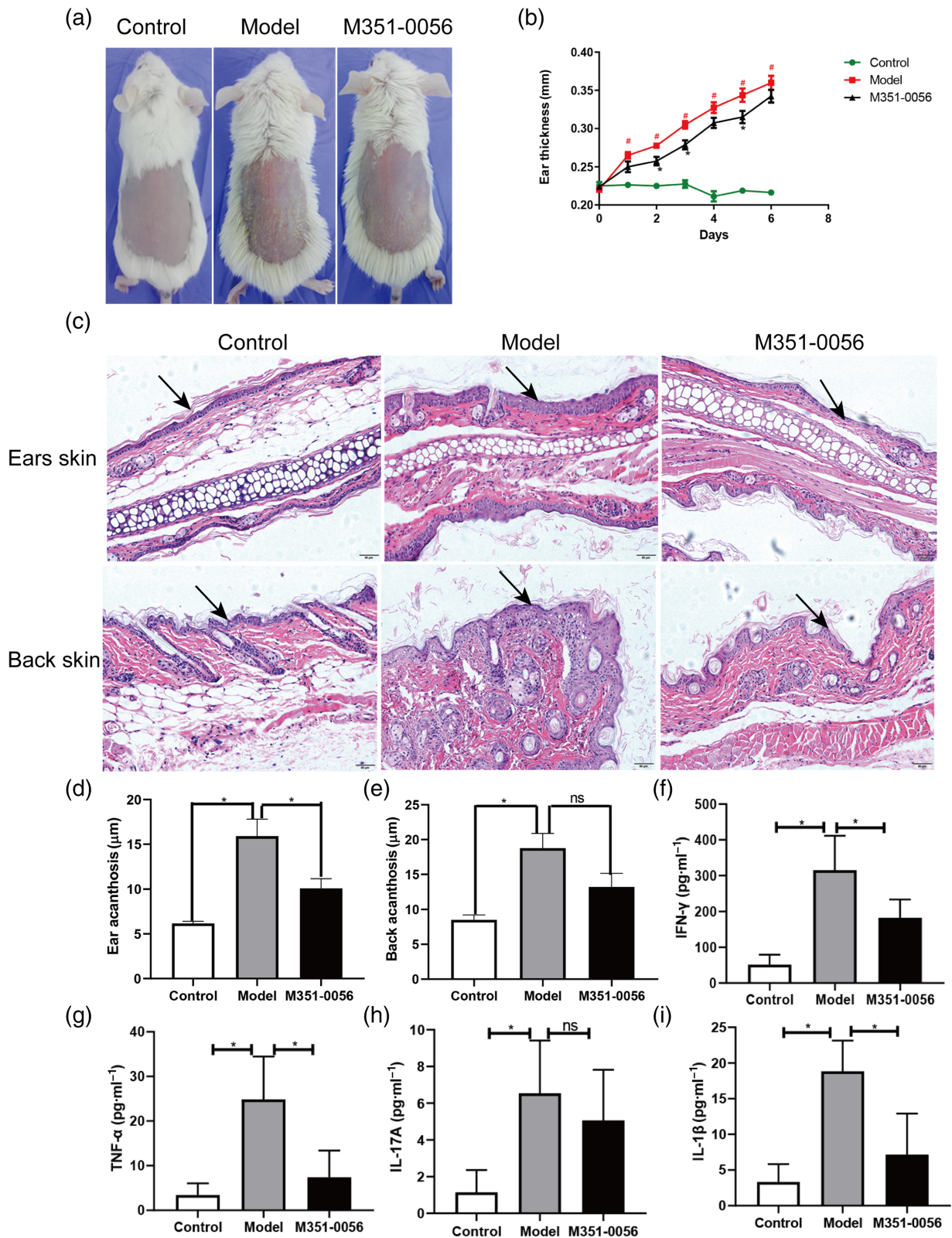
FIGURE 6 M351-0056 improved imiquimod-induced psoriasiform inflammation in BALB/c mice. (a) Efficacy of M351-0056 (25 mg·kg^{-1} once daily) to mice with imiquimod-induced psoriasis. (b) Ear thickness of the different experimental groups was measured daily. $^{\#}P < .05$, significantly different from control. $^{*}P < .05$, significantly different from model (imiquimod only). (c) H&E staining of the ear skin (upper panel) and back skin (lower panel) of mice; scale bar 50 μm (×200). On Day 6, ears and back skin were harvested and processed for H&E staining. A representative image of ear skin is shown in (d), and an image of back skin is shown in (e). Serum levels of (f) IFN-γ, (g) TNF-α, (h) IL-17A, and (i) IL-1β in BALB/c mice were assayed by ELISA. Data are given as means ± SD ($n = 8$). $^{*}P < .05$, significantly different, ns, not significant, as indicated
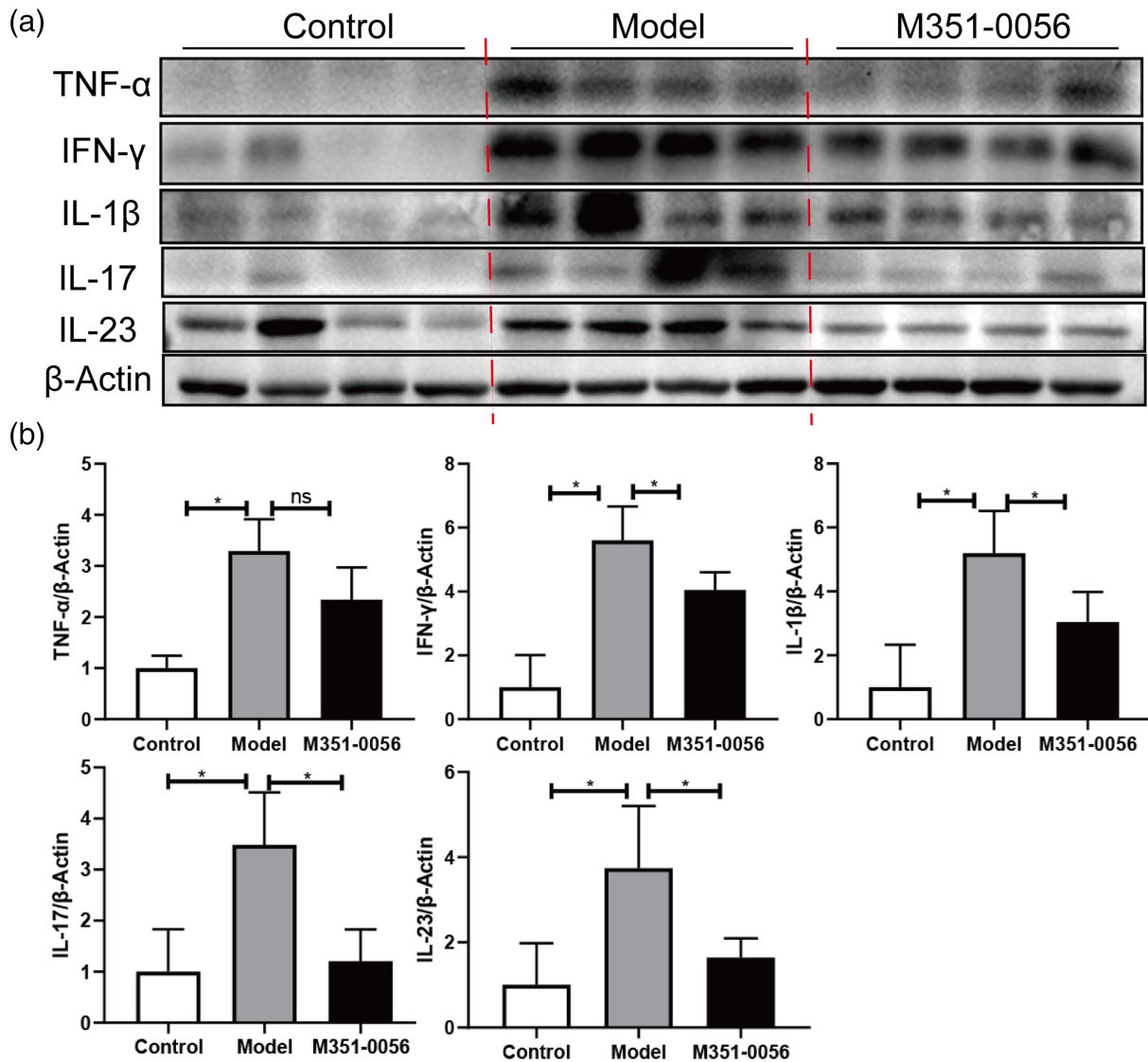
FIGURE 7   M351-0056 decreased expression of inflammatory cytokines (IFN-γ, TNF-α, IL-1β, IL-17, and IL-23) in imiquimod-induced psoriasiform dermatitis in BALB/c mice. (a) The expression of IFN-γ, TNF-α, IL-1β, IL-17, and IL-23 protein were analysed by western blot, in skin from back lesions. (b) The fold change was calculated based on the densitometric analysis of band intensities in western blot. β-Actin was used as an internal control. Data are shown as the means ± SD (n = 8). *P < .05, significantly different, ns, not significant, as indicated

results indicated that M351-0056 targeted VISTA and potentiated its actions, possibly though the JAK2–STAT2 signalling pathway, which is involved in T-cell proliferation.

Psoriasis is one of the most common autoimmune diseases (Lowes, Bowcock, & Krueger, 2007). VISTA deficiency accelerated disease development in the imiquimod-induced model of psoriasis in mice. Although the role played by VISTA in human skin diseases has not yet been analysed in detail, VISTA is an immune check-point regulator known to be important in the maintenance of skin homeostasis and inflammation. Recently, our research has shown that the number of macrophages, fibroblasts, and dendritic cells in VSIR$^{-/-}$ murine psoriasis was significantly increased (Qie et al., 2020), which provides new ideas for studying the function of

VISTA in psoriasis. The mouse model experiments also showed that M351-0056 was effective and safe and ameliorated imiquimod-induced skin inflammation in mice that phenotypically resembles psoriasis. Administration of M351-0056 significantly decreased the serum level of inflammatory cytokines (IFN-γ, IL-17A, TNF-α, and IL-1β) and the expression of mRNA and protein of several pro-inflammatory factors (IFN-γ, IL-17, IL-23, TNF-α, and IL-1β) in mouse psoriasis-like skin tissue.

Therefore, M351-0056 was identified as a new modulator of VISTA. It had higher affinity for the human VISTA protein and could inhibit T-cell activity in vitro and decrease imiquimod -induced skin inflammation in vivo. In this study, the hit ligands identified based on this approach may guide the design of novel low MW modulators of

TABLE 2 Sequence of primers used in the study

	Forward primer (5′-3′)	Reverse primer (5′-3′)
Human PDGFRA	TGGCAGTACCCCATGTCTGAA	CCAAGACCGTCACAAAAGGC
Human IL-4R	ACACCAATGTCTCCGACACTC	TGTTGACTGCATAGGTGAGATGA
Human IL-21R	GGCAAGACCAGTATGAAGAGC	TGACACTGAAAATGTCGTCGG
Human IFNAR1	ATTTACACCATTTCGCAAAGCTC	TCCAAAGCCCACATAACACTATC
Human IFNGR1	TCTTTGGGTCAGAGTTAAAGCCA	TTCCATCTCGGCATACAGCAA
Human JAK2	ATCCACCCAACCATGTCTTCC	ATTCCATGCCGATAGGCTCTG
Human IRF9	GCCCTACAAGGTGTATCAGTTG	TGCTGTCGCTTTGATGGTACT
Human STAT2	CCAGCTTTACTCGCACAGC	AGCCTTGGAATCATCACTCCC
Human PTPN2	GAAGAGTTGGATACTCAGCGTC	TGCAGTTTAACACGACTGTGAT
Human PIAS3	CTTTACCGACGACGCTTTCC	GACTTCATAGAAGGGCAATGGTT
Human GAPDH	GGAGCGAGATCCCTCCAAAAT	GGCTGTTGTCATACTTCTCATGG
Mouse IL-17A	TTTAACTCCCTTGGCGCAAAA	CTTTCCCTCCGCATTGACAC
Mouse TNF-α	CCCTCACACTCAGATCATCTTCT	GCTACGACGTGGGCTACAG
Mouse IFN-γ	ATGAACGCTACACACTGCATC	CCATCCTTTTGCCAGTTCCTC
Mouse GAPDH	AGGTCGGTGTGAACGGATTTG	GGGGTCGTTGATGGCAACA

VISTA and would ultimately benefit patients with safer and more effective therapeutic options for autoimmunity and inflammatory disease.

In conclusion, for the first time, we reported a small-molecule compound modulating VISTA in inflammation. Our findings revealed that the compound M351-0056 has high affinity with VISTA and modulated VISTA function possibly by JAK2–STAT2 pathway. Importantly, compound M351-0056 could ameliorate imiquimod -induced skin inflammation, which provides a promising lead compound for treating autoimmune diseases. Our study indicates that small-molecule compound enhancing the anti-inflammatory function of VISTA may benefit a novel treatment of a variety of inflammatory and autoimmune disorders.

AUTHOR CONTRIBUTIONS

J.L. and X.H. conceived and designed the experiments. X.H., C.Q., J.J., X.X., W.C., and W.L. performed the experiments. X.H., C.Q., and J.J. analysed the data. J.L. and X.H. wrote the paper.

CONFLICT OF INTEREST

The authors declare no conflicts of interest.

DECLARATION OF TRANSPARENCY AND SCIENTIFIC RIGOUR

This Declaration acknowledges that this paper adheres to the principles for transparent reporting and scientific rigour of preclinical research as stated in the *BJP* guidelines for Design & Analysis, Immunoblotting and Immunochemistry, and Animal Experimentation and as recommended by funding agencies, publishers, and other organizations engaged with supporting research.

DATA AVAILABILITY STATEMENT

The data that support the findings of this study are available from the corresponding author upon reasonable request. Some data may not be made available because of privacy or ethical restrictions.

ORCID

Xinlei Hu https://orcid.org/0000-0002-4144-8923

REFERENCES

Alexander, S. P. H., Kelly, E., Mathie, A., Peters, J. A., Veale, E. L., Faccenda, E., ... CGTP Collaborators. (2019). THE Concise Guide to PHARMACOLOGY 2019/20: Other Protein Targets. *British Journal of Pharmacology*, 176, S1–S20. https://doi.org/10.1111/bph.14747

Alexander, S. P. H., Roberts, R. E., Broughton, B. R. S., Sobey, C. G., George, C. H., Stanford, S. C., ... Ahluwalia, A. (2018). Goals and practicalities of immunoblotting and immunohistochemistry: A guide for submission to the *British Journal of Pharmacology*. *British Journal of Pharmacology*, 175(3), 407–411. https://doi.org/10.1111/bph.14112

Anderson, A. C., Joller, N., & Kuchroo, V. K. (2016). Lag-3, Tim-3, and TIGIT: Co-inhibitory receptors with specialized functions in immune regulation. *Immunity*, 44(5), 989–1004. https://doi.org/10.1016/j.immuni.2016.05.001

Andrews, L. P., Marciscano, A. E., Drake, C. G., & Vignali, D. A. (2017). LAG3 (CD223) as a cancer immunotherapy target. *Immunological Reviews*, 276(1), 80–96. https://doi.org/10.1111/imr.12519

Bharaj, P., Chahar, H. S., Alozie, O. K., Rodarte, L., Bansal, A., Goepfert, P. A., ... Shankar, P. (2014). Characterization of programmed death-1 homologue-1 (PD-1H) expression and function in normal and HIV infected individuals. *PLoS ONE*, 9(10), e109103. https://doi.org/10.1371/journal.pone.0109103

Borggrewe, M., Grit, C., Den Dunnen, W. F. A., Burm, S. M., Bajramovic, J. J., Noelle, R. J., ... Laman, J. D. (2018). VISTA expression

by microglia decreases during inflammation and is differentially regulated in CNS diseases. *Glia*, *66*(12), 2645–2658. https://doi.org/10.1002/glia.23517

Ceeraz, S., Eszterhas, S. K., Sergent, P. A., Armstrong, D. A., Ashare, A., Broughton, T., ... Fava, R. A. (2017). VISTA deficiency attenuates antibody-induced arthritis and alters macrophage gene expression in response to simulated immune complexes. *Arthritis Research & Therapy*, *19*(1), 270. https://doi.org/10.1186/s13075-017-1474-y

Ceeraz, S., Sergent, P. A., Plummer, S. F., Schned, A. R., Pechenick, D., Burns, C. M., & Noelle, R. J. (2017). VISTA deficiency accelerates the development of fatal murine lupus nephritis. *Arthritis & Rhematology*, *69*(4), 814–825. https://doi.org/10.1002/art.40020

Chen, L., & Flies, D. B. (2013). Molecular mechanisms of T cell co-stimulation and co-inhibition. *Nature Reviews. Immunology*, *13*(4), 227–242. https://doi.org/10.1038/nri3405

Curtis, M. J., Alexander, S., Cirino, G., Docherty, J. R., George, C. H., Giembycz, M. A., ... Ahluwalia, A. (2018). Experimental design and analysis and their reporting II: Updated and simplified guidance for authors and peer reviewers. *British Journal of Pharmacology*, *175*(7), 987–993. https://doi.org/10.1111/bph.14153

ElTanbouly, M. A., Zhao, Y., Nowak, E., Li, J., Schaafsma, E., Le Mercier, I., ... Huang, X. (2020). VISTA is a checkpoint regulator for naïve T cell quiescence and peripheral tolerance. *Science*, *367*(6475), eaay0524. https://doi.org/10.1126/science.aay0524

Flies, D. B., Wang, S., Xu, H., & Chen, L. (2011). Cutting edge: A monoclonal antibody specific for the programmed death-1 homolog prevents graft-versus-host disease in mouse models. *Journal of Immunology*, *187*(4), 1537–1541. https://doi.org/10.4049/jimmunol.1100660

Gabr, M. T., & Gambhir, S. S. (2020). Discovery and optimization of small-molecule ligands for V-domain Ig suppressor of T-cell activation (VISTA). *Journal of the American Chemical Society*, *142*(38), 16194–16198. https://doi.org/10.1021/jacs.0c07276

Gavrieli, M., Sedy, J., Nelson, C. A., & Murphy, K. M. (2006). BTLA and HVEM cross talk regulates inhibition and costimulation. *Advances in Immunology*, *92*, 157–185.

Greenwald, R. J., Freeman, G. J., & Sharpe, A. H. (2005). The B7 family revisited. *Annual Review of Immunology*, *23*, 515–548. https://doi.org/10.1146/annurev.immunol.23.021704.115611

He, H. Q., Liu, B. Q., Luo, H. Y., Zhang, T. T., & Jiang, J. W. (2020). Big data and artificial intelligence discover novel drugs targeting proteins without 3D structure and overcome the undruggable targets. *Stroke and Vascular Neurology*svn-2019-000323, *5*, 381–387. https://doi.org/10.1136/svn-2019-000323

Janakiram, M., Shah, U. A., Liu, W., Zhao, A., Schoenberg, M. P., & Zang, X. (2017). The third group of the B7-CD28 immune checkpoint family: HHLA2, TMIGD2, B7x, and B7-H3. *Immunological Reviews*, *276*(1), 26–39. https://doi.org/10.1111/imr.12521

Li, N., Xu, W., Yuan, Y., Ayithan, N., Imai, Y., Wu, X., ... Wang, L. (2017). Immune-checkpoint protein VISTA critically regulates the IL-23/IL-17 inflammatory axis. *Scientific Reports*, *7*(1), 1485. https://doi.org/10.1038/s41598-017-01411-1

Lilley, E., Stanford, S. C., Kendall, D. E., Alexander, S. P., Cirino, G., Docherty, J. R., ... Ahluwalia, A. (2020). ARRIVE 2.0 and the *British Journal of Pharmacology*: Updated guidance for 2020. *British Journal of Pharmacology*, 3611–3616. https://doi.org/10.1111/bph.15178

Lines, J. L., Pantazi, E., Mak, J., Sempere, L. F., Wang, L., O'Connell, S., ... Noelle, R. (2014). VISTA is an immune checkpoint molecule for human T cells. *Cancer Research*, *74*(11), 1924–1932. https://doi.org/10.1158/0008-5472.CAN-13-1504

Lines, J. L., Sempere, L. F., Broughton, T., Wang, L., & Noelle, R. (2014). VISTA is a novel broad-spectrum negative checkpoint regulator for cancer immunotherapy. *Cancer Immunology Research*, *2*(6), 510–517. https://doi.org/10.1158/2326-6066.CIR-14-0072

Lowes, M. A., Bowcock, A. M., & Krueger, J. G. (2007). Pathogenesis and therapy of psoriasis. *Nature*, *445*(7130), 866–873. https://doi.org/10.1038/nature05663

Mehta, N., Maddineni, S., Mathews, I. I., Sperberg, R. A. P., Huang, P. S., & Cochran, J. R. (2019). Structure and functional binding epitope of V-domain Ig suppressor of T cell activation. *Cell Reports*, *28*(10), 2509–2516.e5

Percie du Sert, N., Hurst, V., Ahluwalia, A., Alam, S., Avey, M. T., Baker, M., ... Würbel, H. (2020). The ARRIVE guidelines 2.0: Updated guidelines for reporting animal research. *PLoS Biology*, *18*(7), e3000410. https://doi.org/10.1371/journal.pbio.3000410

Qie, C. X., Jiang, J. W., Liu, W. M., Hu, X. L., Chen, W. T., Xie, X. X., & Liu, J. (2020). Single-cell RNA-Seq reveals the transcriptional landscape and heterogeneity of skin macrophages in $Vsir^{-/-}$ murine psoriasis. *Theranostics*, *10*(23), 10483–10497. https://doi.org/10.7150/thno.45614

Wang, L., Le Mercier, I., Putra, J., Chen, W., Liu, J., Schenk, A. D., ... Noelle, R. J. (2014). Disruption of the immune-checkpoint VISTA gene imparts a proinflammatory phenotype with predisposition to the development of autoimmunity. *Proceedings of the National Academy of Sciences of the United States of America*, *111*(41), 14846–14851. https://doi.org/10.1073/pnas.1407447111

Wang, L., Rubinstein, R., Lines, J. L., Wasiuk, A., Ahonen, C., Guo, Y., ... Noelle, R. J. (2011). VISTA, a novel mouse Ig super family ligand that negatively regulates T cell responses. *The Journal of Experimental Medicine*, *208*(3), 577–592. https://doi.org/10.1084/jem.20100619

Yi, K. H., & Chen, L. (2009). Fine tuning the immune response through B7-H3 and B7-H4. *Immunological Reviews*, *229*(1), 145–151. https://doi.org/10.1111/j.1600-065X.2009.00768.x

Zou, W., & Chen, L. (2008). Inhibitory B7-family molecules in the tumour microenvironment. *Nature Reviews. Immunology*, *8*(6), 467–477. https://doi.org/10.1038/nri2326

SUPPORTING INFORMATION

Additional supporting information may be found online in the Supporting Information section at the end of this article.

How to cite this article: Hu X, Qie C, Jiang J, et al. M351-0056 is a novel low MW compound modulating the actions of the immune-checkpoint protein VISTA. *Br J Pharmacol*. 2021; 178:1445–1458. https://doi.org/10.1111/bph.15357